Thermoreflectance Imaging of Superlattice Micro Refrigerators

James Christofferson, Daryoosh Vashaee, Ali Shakouri*
Jack Baskin School of Engineering, University of California, Santa Cruz, CA 95064

Philip Melese
SRI International, Menlo Park, CA 94025

Xiaofeng Fan, Gehong Zeng, Chris Labounty, and John E. Bowers
Electrical and Computer Engineering, University of California, Santa Barbara, CA 93106

Edward T. Croke III
HRL Laboratories Inc.

* Tel. (831) 459-3821, FAX (831) 459-4829, ali@cse.ucsc.edu

Abstract

High resolution thermal images of semiconductor micro refrigerators are presented. Using the thermoreflectance method and a high dynamic range PIN array camera, thermal images with 50mK temperature resolution and high spatial resolution are presented. This general method can be applied to any integrated circuit, and can be used as a tool for identifying fabrication failures. With further optimization of the experimental setup, we expect to obtain thermal images with sub-micron spatial resolution.

Introduction

For various applications in optoelectronic or high power electronic devices, it is useful to control the temperature on a microscopic scale. For example, semiconductor lasers used in wavelength division multiplexed fiber optics communication systems require less than a degree centigrade variation in their operating temperature in order to have stable wavelength and output power. The traditional thermoelectric effect that can provide cooling at the interface between two materials can be enhanced using thermionic emission in superlattice barriers [1,2]. By integrating these heterostructure integrated thermionic (HIT) micro coolers with lasers, and other opto-electronic devices, we can have active temperature control on a small scale thus improving the reliability of thermally sensitive components. Room temperature thermocouple measurements show 4 degrees centigrade of cooling on the surface of the cooler. However, since the size of the micro-coolers can be smaller then the thermocouple, and the measurement is effected by the thermal mass of the thermocouple, non-contact high-resolution characterization methods are preferred.

Thermoreflectance techniques

Many experiments have used the thermoreflectance method for thermal measurements on a microscopic scale. In particular experiments by Goodson[3], Quintard[4] and Claeys[5] have shown good single point results on metal trace experiments and also several experiments by Mansares[6] and Batista[7] have shown thermal imaging with a scanning method. The thermoreflectance technique exploits the change in the reflection coefficient of material with temperature. Using visible wavelength one can achieve submicron spatial resolution.

It is known that the reflection coefficient has a small linear dependence on temperature. The normalized change in reflection per unit temperature is called the thermoreflectance constant and is denoted by C_{th}.

$$C_{th} = (1/R)(dR/dT)$$

C_{th} is 1.5e-4 for silicon and around 1e-5 for metals.

Because of the small temperature dependence of the reflection coefficient, we must modulate the temperature and use heterodyne filtering. We excite the sample with a current pulse, and as long as the excitation period is long enough for the device to reach thermal equilibrium, the magnitude of the oscillation in the reflected light at the excitation frequency is proportional to the change in temperature.

The reflection coefficient of the sample is the initial reflection coefficient at ambient, R_0, plus the change from a change in temperature.

$$R(T)=R_0 + dR/dT * \Delta T$$

Let P_{ref} be the power reflected of the sample, and acquired by the photo detector, or pixel and P_{in} be the optical power incident on the sample.

$$P_{ref}= P_{in}R_0 + P_{in}\, dR/dT * \Delta T$$

Let us assume that ΔT is periodic at some excitation frequency ω. Let P_ω be the power at the excitation frequency that we recover through heterodyne filtering.

Report Documentation Page

Form Approved
OMB No. 0704-0188

1. REPORT DATE	2. REPORT TYPE	3. DATES COVERED
2006		**00-00-2006 to 00-00-2006**

4. TITLE AND SUBTITLE	5a. CONTRACT NUMBER
Thermoreflectance Imaging of Suprelattice Micro Refrigerators	5b. GRANT NUMBER
	5c. PROGRAM ELEMENT NUMBER
6. AUTHOR(S)	5d. PROJECT NUMBER
	5e. TASK NUMBER
	5f. WORK UNIT NUMBER
7. PERFORMING ORGANIZATION NAME(S) AND ADDRESS(ES) **Baskin School of Engineering,University of California,Santa Cruz,CA,95064**	8. PERFORMING ORGANIZATION REPORT NUMBER
9. SPONSORING/MONITORING AGENCY NAME(S) AND ADDRESS(ES)	10. SPONSOR/MONITOR'S ACRONYM(S)
	11. SPONSOR/MONITOR'S REPORT NUMBER(S)

12. DISTRIBUTION/AVAILABILITY STATEMENT
Approved for public release; distribution unlimited

13. SUPPLEMENTARY NOTES
The original document contains color images.

14. ABSTRACT

15. SUBJECT TERMS

16. SECURITY CLASSIFICATION OF:			17. LIMITATION OF ABSTRACT	18. NUMBER OF PAGES	19a. NAME OF RESPONSIBLE PERSON
a. REPORT	b. ABSTRACT	c. THIS PAGE			
unclassified	**unclassified**	**unclassified**		**5**	

$P_\omega = P_{in} * dR/dT * \Delta T$

Using the definition of the thermoreflectance constant, the change in temperature is

$\Delta T = P_\omega/(P_{in}*R_0*C_{th})$

But $P_{in}*R_0$ is simply the unmodulated, DC reflectivity of the sample. Therefore, the experimentally obtained change in temperature is the modulated signal divided by the normalization, which is the DC magnitude, times the thermoreflectance constant.

The thermal resolution depends on several factors; amount of incident light reflected off the sample, value of C_{th}, how large is the area we are measuring, and also the bandwidth window resulting from the heterodyne filtering. The amount of thermal signal compared to the fundamental shot and Johnson noise, dictates the overall thermal resolution. In practice, for an area corresponding to $10\mu m^2$ of the device, we have about 1μA photocurrent, of which only 10pA is the modulated thermoreflectance signal. Thus for good signal to noise, we need to perform a 30 second FFT, corresponding to a .033Hz window.

Experimental Setup

The simple experimental setup is shown in figure 1. A white light from a fiber-optic illuminator is reflected off the sample, and the enlarged image of the device is collected by the camera.

To generate a thermal image, the amount of thermoreflectance signal is normalized to the total amount of light on the surface of the device. This means our thermal camera must have a dynamic range on the order of the thermoreflectance constant (10^{-5}-10^{-6}). Because of this, a standard CCD cannot be used. To capture thermal images, we need a camera with high dynamic range and enough sensitivity to capture the small thermoreflectance signal. A few experiments have tried to use a traditional CCD[8,9] for capturing thermal images, but such experiments were only sensitive to changes of 10's of degrees.

At SRI International a camera has been developed that can be used to capture thermal images. Each pixel of the SRI camera receives different gain for the AC and DC signal, then is heterodyne filtered with a fast Fourier transform (FFT). The camera is based on the Hamamatsu 16x16 PIN array detector.

The main advantage comparing to conventional infrared cameras is the improved spatial resolution. Typical HgCdTe-based cameras have a diffraction limited spatial resolution of 3-5 microns, while visible wavelength thermoreflectance imaging can give submicron resolution. On the other hand, the cooling or heating over small areas can be measured accurately without the effect of background radiation. For example at very low ambient temperatures, there is not enough blackbody radiation to measure the device performance.

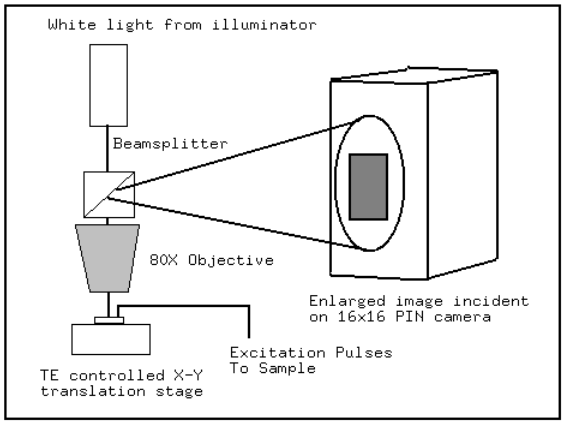

Figure1: Experimental Setup.

Processing the Images

Generating thermal images from the raw data, consists of normalization, correcting for different materials' C_{th} values, and determining the heating and cooling points.

Normalization consists of simply accounting for the total amount of light that is reflected and can be accomplished by simply dividing the thermoreflectance image, by the DC, or normalization image. This should also account for variations in responsivity at different pixels of the camera.

Next, different reflection surfaces must be accounted for different thermoreflectance constants. Each material has a different C_{th} and therefore to obtain an accurate thermal image, different values are assigned to different reflection surfaces. In the micro-refrigerator images, there is only the gold reflection surface, and also silicon. This can almost be corrected automatically, as the histogram of the normalization image is bi-modal, due to a lower overall reflectivity of silicon.

Finally we must determine which points in the image are heating and cooling. From the FFT we know the overall magnitude of the thermal signal, but we must look at the phase image to know if the thermal change is positive or negative. This is exacerbated by the fact that our camera introduces a slight phase difference per pixel because the channels are not read exactly in parallel. This operation can be automated, provided that the user input the dominant phase.

Experimental Results

The geometry of the micro cooler samples is show in figure 2. Images of a 10x10micron operating micro refrigerator are presented. Figure 3 shows the normalization image of the cooler. The image is interpolated from the 16x16 pixels of the SRI camera. Figure 4 shows the thermal image, and Figure 6 its contour plot. Approximately 3 degrees centigrade of cooling on the top surface of the cooler is demonstrated.

In figure 6 we see an image of a different micro cooler and a current probe on top of the device. In this batch of samples there is no side metallic contact. The current probe, in the forground of figure 6, sits directly on top of a 100x180 micron rectangular micro refrigerator. As expected, in the thermal image, figure 7, there is excessive heating caused by the current probe. It is interesting to note that there is close to 4 degrees of cooling very near the probe which is caused by

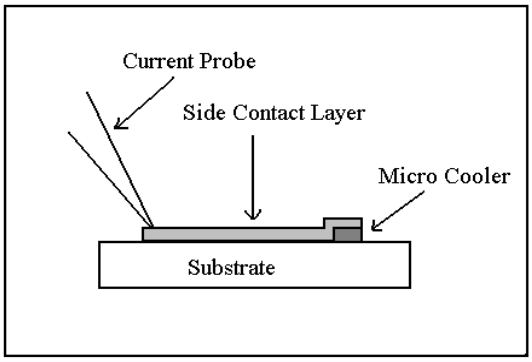

Figure 2: Geometry of Micro Refrigerator Samples

the high cooling density in that area. Previous thermocouple measurements of this device showed less then 2 degrees of cooling, which is what we see over most of the device after the current has spread out. Figure 8 shows a cross section across the device depicting the hot and cool regions of the micro refrigerator. In this image we took the thermoreflectance constant of the current probe material, to be the same as Gold.

Identifying Fabrication Failures

Another useful aspect of the thermal imaging camera is that it can be used to identify fabrication failures. Figure 9 shows a CCD image of a 20x20 μm^2 micro-cooler. The normalization image is shown in figure 10. Two different thermal images of 20x20μm^2 micro coolers are presented at the same operating current. Figure 11 shows a nice cooling distribution across the device, while in figure 12 we see a device that has excessive heating at the boundary between the contact layer to the micro cooler. This has been identified as a problem in the deposition of the metal contact layer. This failure could not be observed by the inspection of CCD images. The cross-section temperature profile of the two devices are shown in figure 13.

Conclusion

Thermoreflectance imaging is used to determine the performance of superlattice micro refrigerators. This is a very sensitive technique that can be used to identify fabrication failures. This method can be applied to other active devices and integrated circuits. Since visible light is used, spatial resolution can be better than commercial IR cameras. With further optimization of the light source and camera, we expect to improve the thermal resolution and achieve real time sub-micron thermal images with 10-20mK temperature resolution.

Acknowledgements

This work was funded by the Packard Foundation and the DARPA Heretic program.

Refrences

1.Ali Shakouri and John E. Bowers, "Heterostructure Integrated Thermionic Coolers", Applied Physics Letters, 71(9), pp. 1234-1236, September 1997.

2. Gehong Zeng; Shakouri, A.; Bounty, C.L.; Robinson, G.; Croke, E.;Abraham, P.; Xiafeng Fan; Reese, H.; Bowers, J.E. "SiGe micro-cooler,"Electronics Letters, vol.35 (24), 25:2146-7, Nov. 1999.

3. K.E. Goodson and Y.S. Ju, "Short-time-scale thermal mapping of microdevices using a scanning thermoreflectance technique," *Trans. of the ASME*, p.306-313, May 1998.

4. Quintard, Dilhaire, Phan, and Claeys. "Temperature measurement of metal lines under current stress by high resolution laser probing," *IEEE Trans. on Instrumentation and Measurement*, p.69-74, Feb 1999.

5. T Phan, S Dilhaire, V Quintard, W Claeys, and J Batsale. "Thermoreflectance measurements of transient temperature upon integrated circuits: application to thermal conductivity identification,"*Microelectronics Journal*, 29:181-190, 1998.

6. A Mansanares, D Fournier, A Boccara. " Temperature measurements of telecommunication lasers on a micrometre scale", *Electronics Letters*, 29(23):2045-2047, 1993.

7. J. Batista, A Mansanares, EC DaSilva, M Pimentel, N Januzzi, D Fournier. "Subsurface microscopy of biased metal oxide semiconductor field effect transistor structures: photothermal and electroreflectance images," *Senors and Actuators A*, 71:40-45, 1998.

8. T Spirig, P Seitz, O Vietze, and F. Heitger. "The lock in ccd, two dimensional synchroneous detection of light," *IEEE Journal of Quantum Electronics*, p.1705-1708, Sept. 1995.

9. S Grauby, S Hole and D Fournier. "High resolution photothermal imaging of high frequency using visible charge couple device camera associated with multichannel lock-in scheme," *Review of Scientific Instruments.* P.3603-3608, Sept.1999.

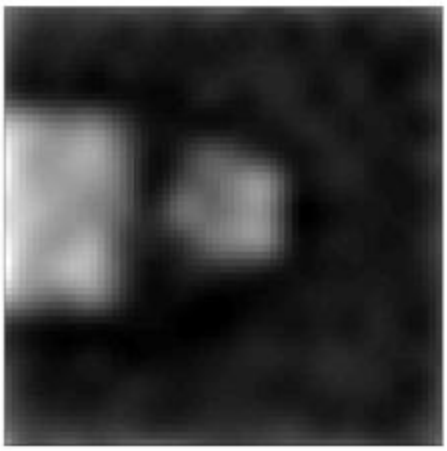

Figure 3: Normalization image of 10x10 micron refrigerator from thermal camera.

Figure 6: Normalization image from thermal camera showing current probe on top of micro refrigerator.

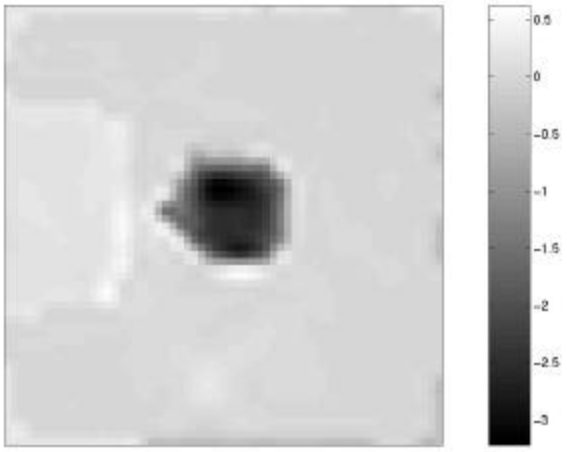

Figure 4: Thermal Image of 10x10 micron refrigerator.

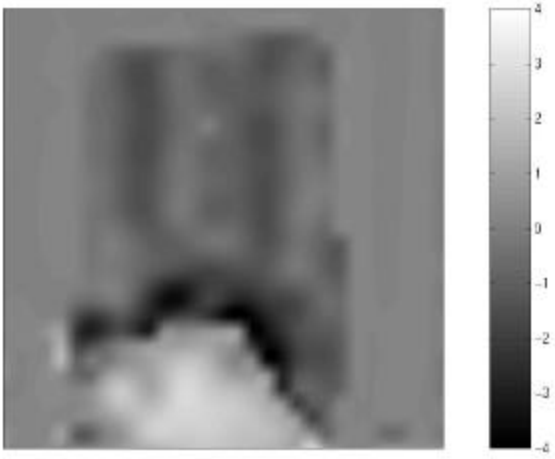

Figure 7: Thermal Image showing heating at current probe and cooling on cooler surface.

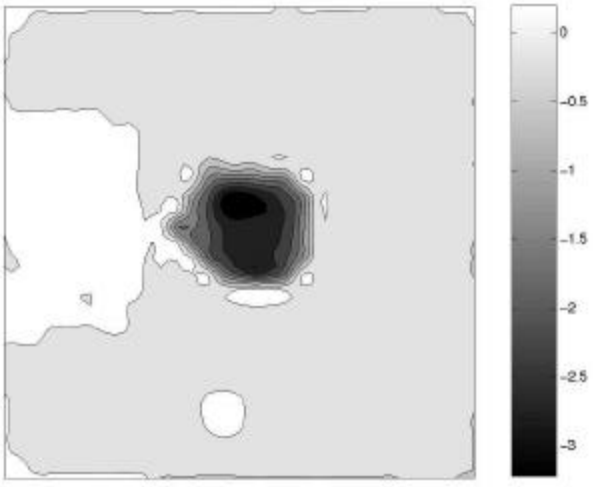

Figure 5: Contour Plot of Thermal Image.

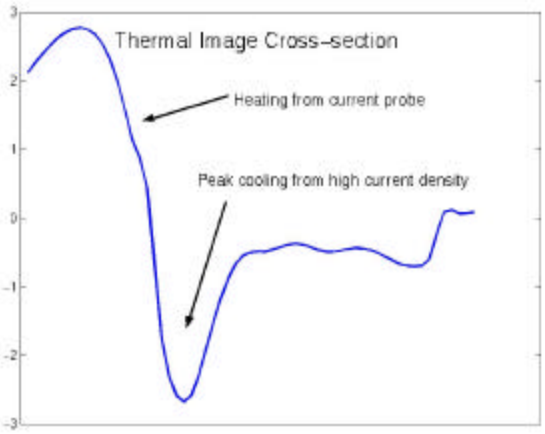

Figure 8: Cross-section of thermal image.

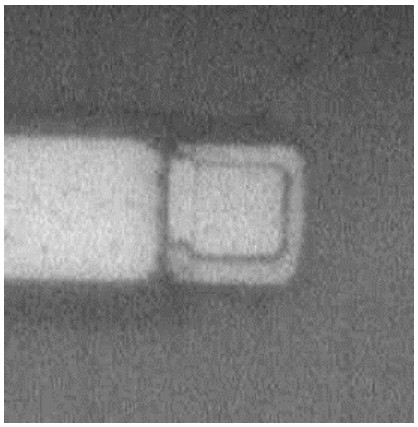

Figure 9: CCD Image of 20x20 micron Micro Refrigerator.

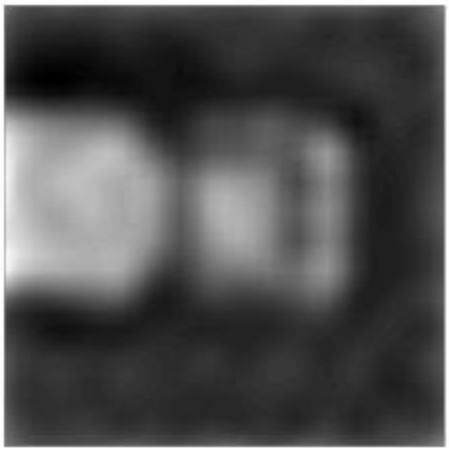

Figure 10: Normalization image seen through the thermal camera.

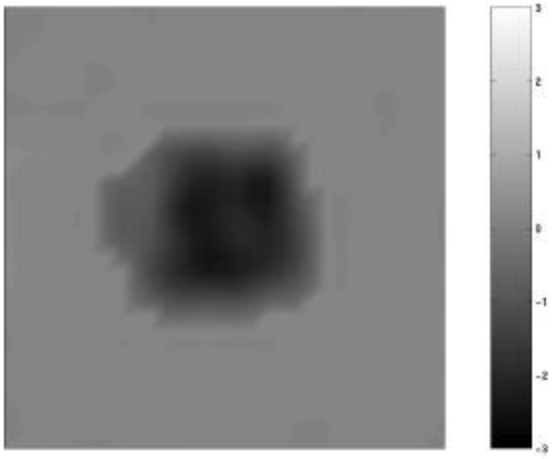

Figure 11: Good Cooling Distribution on well fabricated 20x20 micron device.

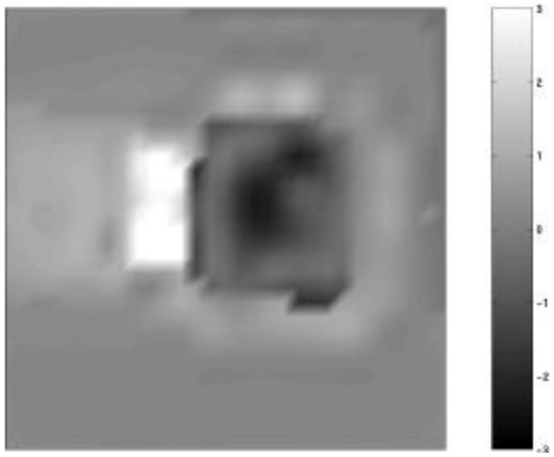

Figure 12: Excessive heating at the boundry from fabrication error.

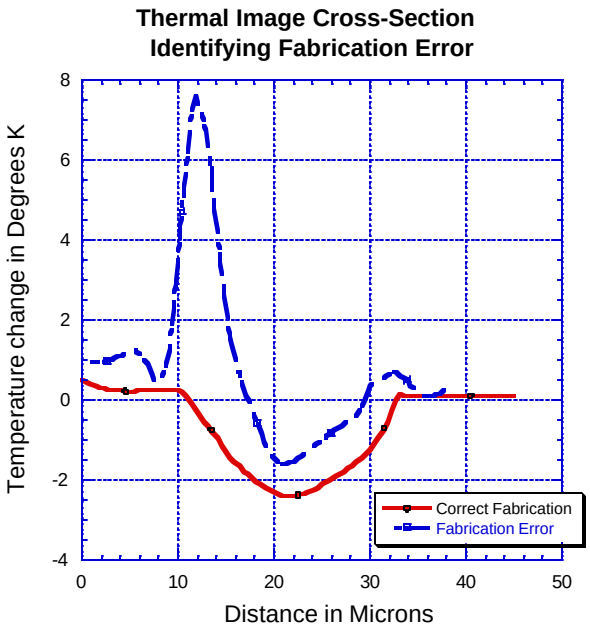

Figure 13: Cross-section plot comparing two 20x20 micron devices.